HHS Public Access

Author manuscript

J Am Soc Cytopathol. Author manuscript; available in PMC 2021 November 01.

Published in final edited form as:

J Am Soc Cytopathol. 2020 ; 9(6): 494–501. doi:10.1016/j.jasc.2020.07.134.

SMARCB1-deficient Carcinomas of the Head and Neck Region: A Cytopathologic Characterization

Brie E Kezlarian, MD[a], **Oscar Lin, MD PhD**[a,*], **Snjezana Dogan, MD**[a,*]

[a]Department of Pathology, Memorial Sloan Kettering Cancer Center, New York, NY, 10065, USA

Abstract

Introduction—*SMARCB1* encodes for a component of the SWI/SNF complex and is widely implicated in carcinogenesis. In the head and neck, SMARCB1-deficient carcinomas typically arise in the sinonasal tract but can be found at other sites. EZH2 inhibitors have emerged as potential targeted therapy against SWI/SNF-deficient tumors. We sought to characterize the cytomorphology of head and neck carcinomas with SMARCB1 deficiencies to identify potential candidates for targeted therapy.

Materials and Methods—Head and neck carcinomas with *SMARCB1* mutations were retrospectively identified and confirmed to be SMARCB1 deficient by both molecular (FISH or Next Generation Sequencing) and immunohistochemical means. Cases with positive cytology were reviewed and their cytologic features cataloged.

Results—A total of 19 specimens from 13 patients were reviewed, including 8 specimens from 7 sinonasal carcinomas, 4 specimens from 3 thyroid carcinomas, 3 specimens from 2 skin carcinomas, and 4 specimens from 1 carcinoma of unknown primary origin. High-grade features were common, including mitoses (11/19) necrosis (13/19) and multinucleation (16/19). Tumors showed either dense cytoplasm with distinct cell borders (10/19) or delicate cytoplasm with indistinct cell borders (9/19). Most tumors showed no distinct epithelial differentiation (12/19), while some (7/19) showed glandular or signet ring features. A minor cohort demonstrated rhabdoid cells (4/19).

Conclusion—Head and neck carcinomas with SMARCB1 deficiencies have a wide array of morphologies and tend to demonstrate high-grade features. Only a minor cohort demonstrate rhabdoid-type cells. Evaluation of SMARCB1 deficiency for potential targeted therapy should not be limited to tumors with rhabdoid morphology.

Corresponding Authors: Oscar Lin, MD, Department of Pathology, Memorial Sloan Kettering Cancer Center, 1275 York Avenue, New York, NY 10065, Tel: (212) 639-2395, LinO@mskcc.org, Snjezana Dogan, MD, Department of Pathology, Memorial Sloan Kettering Cancer Center, 1275 York Avenue, New York, NY 10065, Tel: (212) 639-4878, DoganS@mskcc.org.

*Drs. Lin and Dogan should be considered joint senior authors.

Disclosure of conflict of interest: The Authors have no conflicts of interest to disclose.

Keywords

SMARCB1; INI-1; SWI/SNF; SMARCB1-deficient sinonasal carcinoma; SMARCB1-deficient Carcinoma of Head and Neck

BACKGROUND

The Switch/Sucrose Non-Fermentable (SWI/SNF) protein complex is ubiquitous in tissue and is highly evolutionarily conserved.[1] The overall function of the SWI/SNF complex is to control gene expression through histone modification.[2] In normal development, it is associated with development and differentiation of tissues toward a particular lineage.[1–3] This is accomplished through the interchangeability of the SWI/SNF complex protein subunit modules, allowing for tissue specificity.[1,4,5] Components of SWI/SNF protein complex are involved in regulation of the p16-RB pathway, canonical WNT (β-catenin dependent) pathway, and sonic hedgehog pathway.[2,6]

While many SWI/SNF protein subunits are interchangeable, BAF47 (also known as INI-1 or Integrase Interactor 1 and SNF5) is a required component of all SWI/SNF complexes.[2,6] *SMARCB1* is the gene encoding for this protein, which is located at 22q11.23.[6,7] Since they were first described in malignant rhabdoid tumors,[7] mutations in *SMARCB1* have been associated with many tumor types throughout the body.[2,6,8] Tumors with BAF47 loss and loss of other SWI/SNF proteins are commonly associated with what has been described as a rhabdoid morphology,[7–13] characterized by abundant dense eosinophilic cytoplasm and eccentrically placed nucleus.

In the head and neck region, *SMARCB1* mutations are most commonly associated with a recently described entity known as SMARCB1-deficient sinonasal carcinoma. The first case of an unusual undifferentiated sphenoid tumor harboring *SMARCB1* deletion was reported by Jamshidi *et al*[14] and this was shortly followed by the first two concurrently published case series in 2014.[15,16] Later studies further described the extended morphologic spectrum of these tumors.[17] Three morphologic subgroups were defined, including basaloid, plasmacytoid/rhabdoid, oncocytoid/adenocarcinoma-like pattern, among others.[17,18] Rhabdoid cells were seen in tumors of all morphologic subtypes but in varying proportions.[15,18]

The cytology findings of SMARCB1-deficient sinonasal carcinomas have been previously described in a limited number of cases. The first known case report was published by Allison and colleagues in 2016.[19] The tumor was described as being relatively monomorphic, composed of polygonal to plasmacytoid cells arranged in poorly cohesive clusters. Nuclei were eccentrically located, round to oval, and had prominent nucleoli.[19] Rhabdoid cells were seen, albeit sparsely.[19] This report was followed in 2018 by a series of 6 cases published by Allard and colleagues.[20] The majority of these cases showed a basaloid appearance with indistinct cell borders, but some cases with distinct cell borders were also seen.[20] While moderate anisonucleosis and multinucleation were present in a single case, “overt nuclear pleomorphism” was not seen.[20] Interestingly, the most common feature seen in histology specimens, rhabdoid cells, were only seen in two cases.[20] SMARCB1-deficient

sinonasal carcinomas are not the only tumors of the head and neck known to harbor *SMARCB1* mutations. A large study performed in 2016 investigating the mutational landscape of poorly differentiated and anaplastic thyroid carcinoma demonstrated *SMARCB1* mutations in 6% of anaplastic thyroid carcinomas.[21] Additionally, at our institution, we have detected loss of SMARCB1 protein in other tumors arising in the head and neck region, such as skin.[22]

Detection of tumors with SMARCB1 loss of protein has become increasingly important with the advent of EZH2 inhibiting pharmaceutical compounds as targeted therapy. Studies have demonstrated that the SWI/SNF complex and the Polycomb repressive complex 2 (PRC2) are antagonistic.[1,23,24] SWI/SNF complex has been linked to tissue lineage differentiation,[1–3] whereas PRC2 has been associated with propagation of the stem cell phenotype.[25] It is believed that the unchecked overactivity of PRC2 at its catalytic subunit EZH2 is responsible for the oncogenic potential of SWI/SNF mutations.[24] Multiple *in vitro* studies have demonstrated the efficacy of EZH2 inhibition in SWI/SNF deficient cell lines.[26–29] A phase 2 trial to investigate the *in vivo* efficacy of EZH2 inhibitors as targeted therapy in SWI/SNF depleted tumors is currently underway.[30]

Considering the characteristic morphology of SMARCB1-deficient malignancies reported in the literature[7–13], we hypothesize that SMARCB1-deficient carcinomas may similarly have unifying identifiable morphologic features. Given the potential for EZH2 targeted therapy and the particular amenability to fine needle aspiration biopsy of head and neck lesions, we proposed to analyze the cytomorphologic features of SMARCB1-deficient carcinomas arising in the head and neck.

METHODS

After approval from our Institutional Review Board, the institutional database was queried for tumors with deleterious mutations in *SMARCB1* (INI-1) arising in the head and neck region. A total of 13 cases with available cytology specimens were identified. *SMARCB1* mutation was confirmed on the surgical resection specimen by one of two molecular methods: Fluorescence *in situ* hybridization (FISH) or targeted exome sequencing MSK-IMPACT assay as previously described.[31,32] INI-1 loss was confirmed immunohistochemically on 4 μm formalin-fixed paraffin-embedded tissue sections (BD Biosciences Clone 25; 1:200).

All cytology specimens were reviewed in tandem with available histologic sections by three board-certified pathologists, including 22 Diff-Quik stained smears, 9 Pap stained smears, 5 H&E stained smears, 13 ThinPrep slides, and 16 formalin-fixed, paraffin-embedded cell block slides. Cytologic preparations were reviewed for a panel of cytomorphologic features, including background findings, presence of necrosis, architectural patterns, quality of cell borders (distinct or indistinct), degree of cohesion (discohesive, loosely cohesive, or cohesive), cellular morphology, cell size (small, intermediate or large), variation in cell size (described as a ratio of smallest:largest), quantity of cytoplasm (scant, moderate or abundant), cytoplasmic quality (dense to delicate), presence of eosinophilic cytoplasmic globules, presence of vacuoles, chromatin pattern, presence of nuclear grooves and/or

indentations, size of nucleoli (small to prominent), number of nucleoli, presence of mitoses, multinucleation and cellular differentiation.

RESULTS

Our cohort consisted of 19 cytology specimens from 13 patients. Our patient population included 7 men and 6 women ranging in age from 33–79 (mean age 53). The tumors consisted of 7 SMARCB1-deficient sinonasal carcinomas, 3 thyroid carcinomas, 2 carcinomas primary to the skin, and 1 tumor of unknown primary initially identified in a level 2 neck lymph node. Two of the thyroid carcinomas were diagnosed as anaplastic, while the third was diagnosed as an undifferentiated malignant neoplasm arising in association with a papillary thyroid carcinoma, cribriform morular variant. (Table 1) The cells were present in clusters as well as single cells in the cytology preparations. Cells were round, polygonal, or plasmacytoid with cytoplasmic quantity ranging from scant to abundant. There was also great variability with respect to anisocytosis, ranging from 1:2 to 1:20 size variation. Mitoses (11/19) and necrosis (13/19) were common. Nuclei often showed grooves or indentations (13/19) with coarse to vesicular chromatin. Nucleoli were universally present (19/19) and were either small (13/19) or prominent (6/19). Nucleoli number ranged from 1 to over 5. Focal multinucleation was a common finding and was identified in 16/19 cases. (Figure 1)

With respect to cellular differentiation, the most common finding was no distinct epithelial differentiation (12/19), while a minority (7/19) showed glandular or signet ring differentiation. Cells with rhabdoid features were seen in 4/19 of cases. (Figure 2) Of note, the cytoplasmic inclusions of rhabdoid cells appeared teal to blue in Papanicolaou stained preparations. Glandular differentiation and rhabdoid morphology were not mutually exclusive, with both present in 2/19 cases. Vacuoles were present in 13/19 of cases. Round eosinophilic cytoplasmic densities were seen in 4/19 of cases. Similar to the rhabdoid inclusions, these densities appeared blue on Papanicolaou stained preparations. (Figure 3)

Although our analysis showed a spectrum of morphologic findings, tumors could be subdivided into one of two major morphologic patterns. They showed either delicate cytoplasm with indistinct cell borders (47%) or dense cytoplasm with distinct cell borders (53%). (Figure 4)

DISCUSSION

The ability to identify carcinomas with potential *SMARCB1* mutations takes on special significance in light of EZH2 inhibitory targeted therapy. Our study demonstrates that one must not limit consideration for potential use of this therapeutic agent to SMARCB1-deficient sinonasal carcinomas alone. While many cases in our cohort were SMARCB1-deficient sinonasal carcinomas, 46% were other histotypes. In addition to SMARCB1-deficient sinonasal carcinomas, poorly differentiated and anaplastic thyroid carcinomas have been previously reported to harbor *SMARCB1* mutations. Additionally, 2 novel cases of SMARCB1-deficient carcinomas of the skin have recently been reported by our group[22], the cytologic features of which are described herein. If EZH2 inhibitor therapy proves to be

efficacious against head and neck tumors with *SMARCB1* mutations, any tumor with high-grade features or multinucleation on cytology arising in this region should be considered a candidate for SMARCB1 assessment.

The main aim of our study was to characterize the cytomorphologic features of SMARCB1-deficient carcinomas arising in the head and neck region, as lesions in these areas are often amenable to fine needle aspiration biopsies. The tumors in our cohort tended to show high-grade features, which was congruent with their histologic characteristics. Mitoses (58%) and necrosis (68%) were identified in the majority of cases. Multinucleation (89%) and anisocytosis were also present in the majority of the cases. There was a significant degree of heterogeneity in our cohort, likely due in part to the variation in tumor classification. Despite this morphologic heterogeneity, tumors could be subdivided into one of two major morphologic patterns. They showed either delicate cytoplasm with indistinct cell borders (47%) or dense cytoplasm with distinct cell borders (53%). No discernable pattern was identified among tumor types for all observed characteristics. This finding should be interpreted with caution the relatively small sample size for individual tumor types.

Previous investigation into the cytologic features of carcinomas with SMARCB1 deficiency in the head and neck region is limited to 7 SMARCB1-deficient sinonasal carcinomas.[19,20] Similar to our cohort, these studies identified high grade features, including frequent necrosis and mitotic figures. These studies also found rhabdoid cells in only a subset (3/7) of cases. Our findings differed with respect to anisocytosis. We had significant anisocytosis in our cohort, whereas previous studies found 6/7 cases showed a uniform population of cells, with 1/7 showing only moderate variation. We identified multinucleation in 16/19 cases. Multinucleation was only noted in 1/7 previously reported cases. These differences might be attributed to the larger number of cases in our cohort.

SWI/SNF mutations have long been associated with a rhabdoid phenotype in the literature.[7–9,11–13] Rhabdoid cells are defined as having dense eosinophilic inclusions found to be composed of intermediate filaments[33] which displace the nucleus eccentrically. Our study demonstrates that while classic rhabdoid cells can be seen in these tumors, they were not the predominant morphological finding. Of interest, we identified dense eosinophilic cytoplasmic globules in 4 of 19 cases, which were found to coexist with rhabdoid cells in 2 cases. These globules could be analogous to the inclusions identified in classical rhabdoid cells but are not large enough to displace the nucleus eccentrically to complete the rhabdoid appearance. Alternatively, these globules could represent condensation of these intermediate filaments. Further study may be warranted to interrogate this relationship, if one exists.

All thyroid carcinomas identified to have *SMARCB1* mutations in our institutional query were diagnosed as anaplastic carcinomas, or as an undifferentiated neoplasm admixed with cribriform morular variant of papillary thyroid carcinoma. The acquisition of SWI/SNF mutations has been associated with dedifferentiation at other tumor sites, particularly in endometrial carcinomas.[13,34,35] Given the lack of differentiation not only in the thyroid specimens, but the majority of specimens in our cohort and given the association of SWI/SNF proteins with tissue lineage differentiation, one must consider if the loss of

SMARCB1 and other SWI/SNF proteins contributes to an undifferentiated tumor phenotype regardless of tissue of origin.

Both anaplastic thyroid carcinomas showed coexisting (likely) oncogenic mutations in addition to *SMARCB1*[21]. Among them, one anaplastic thyroid carcinoma showed a *BRAF* V600E and a *TERT* promoter mutation suggesting that *SMARCB1* mutation in these carcinomas may not necessarily represent an initiating driver alteration. Importantly, this study demonstrates one must consider thyroid origin when confronted with a SMARCB1-deficient undifferentiated appearing neoplasm.

One may consider the heterogeneity of tumor types to be a limitation of this study. Indeed, the variation in tumor types likely accounts for a significant amount of the heterogeneity in morphologic features. However, the purpose of this study was to identify unifying morphologic characteristics due to a molecular alteration independent of tumor type. With this goal in mind, the tumor type heterogeneity may underscore the validity of our findings with respect to the morphologic similarities observed between these tumors.

Analysis of the prevalence of *SMARCB1* mutations in tumors of the head and neck region was not the subject of this study. Only tumors for which a *SMARCB1* mutation was identified were retrospectively identified to include in our cohort. Additionally, this study was performed at a large cancer hospital, and therefore subject to referral bias.

CONCLUSION

Our study demonstrates that the cytomorphologic features of SMARCB1-deficient carcinoma are variable, tend to show high-grade features, and frequently demonstrate multinucleation. Morphologically, they can be subdivided into two major categories- either delicate cytoplasm with indistinct cell borders or dense cytoplasm with distinct cell borders. Importantly, not all cases demonstrated the presence of rhabdoid cells. Evaluation of SMARCB1 deficiency for potential targeted therapy should not be limited to tumors with rhabdoid morphology. Rather, any high-grade carcinoma should be considered a potential candidate for *SMARCB1* mutation analysis, particularly if multinucleation is present.

Funding Statement:

Research reported in this publication was supported in part by the Cancer Center Support Grant of the National Institutes of Health/National Cancer Institute under award number P30CA008748. The content is solely the responsibility of the authors and does not necessarily represent the official views of the National Institutes of Health.

REFERENCES

1. Alver BH, Kim KH, Lu P, et al. The SWI/SNF chromatin remodelling complex is required for maintenance of lineage specific enhancers. Nat Publ Gr. 2017;8:1–10. doi:10.1038/ncomms14648
2. Wilson BG, Roberts CWM. SWI/SNF nucleosome remodellers and cancer. Nat Rev Cancer. 2011;11(7):481–492. doi:10.1038/nrc3068 [PubMed: 21654818]
3. Sokpor G, Xie Y, Rosenbusch J, Tuoc T. Chromatin Remodeling BAF (SWI/SNF) Complexes in Neural Development and Disorders. Front Mol Neurosci. 2017;10(August):1–22. doi:10.3389/fnmol.2017.00243 [PubMed: 28167898]

4. Kadoch C, Crabtree GR. Mammalian SWI/SNF chromatin remodeling complexes and cancer: Mechanistic insights gained from human genomics. Sci Adv. 2015;1(5):e1500447. doi:10.1126/sciadv.1500447 [PubMed: 26601204]
5. Mashtalir N, Avino ARD, Michel BC, Cassel SH, Ranish JA, Kadoch C. Modular Organization and Assembly of SWI / SNF Family Chromatin Remodeling Complexes Article Modular Organization and Assembly of SWI / SNF Family Chromatin Remodeling Complexes. Cell. 2018;175(5):1272–1288.e20. doi:10.1016/j.cell.2018.09.032 [PubMed: 30343899]
6. Kohashi K, Oda Y. Oncogenic roles of SMARCB1/INI1 and its deficient tumors. Cancer Sci. 2017;108(4):547–552. doi:10.1111/cas.13173 [PubMed: 28109176]
7. Versteege I, Sévenet N, Lange J, et al. Truncating mutations of hSNF5/INI1 in aggressive paediatric cancer. Nature. 1998;394(6689):203–206. doi:10.1038/28212 [PubMed: 9671307]
8. Hollmann TJ, Hornick JL. INI1-deficient tumors: Diagnostic features and molecular genetics. Am J Surg Pathol. 2011;35(10):47–63. doi:10.1097/PAS.0b013e31822b325b
9. Sauter JL, Graham RP, Larsen BT, Jenkins SM, Roden AC, Boland JM. SMARCA4-deficient thoracic sarcoma: A distinctive clinicopathological entity with undifferentiated rhabdoid morphology and aggressive behavior. Mod Pathol. 2017;30(10):1422–1432. doi:10.1038/modpathol.2017.61 [PubMed: 28643792]
10. Witkowski L, Goudie C, Foulkes WD, McCluggage WG. Small-Cell Carcinoma of the Ovary of Hypercalcemic Type (Malignant Rhabdoid Tumor of the Ovary). A Review with Recent Developments on Pathogenesis. Surg Pathol Clin. 2016;9(2):215–226. doi:10.1016/j.path.2016.01.005 [PubMed: 27241105]
11. Agaimy A, Haller F, Frohnauer J, et al. Pancreatic undifferentiated rhabdoid carcinoma: KRAS alterations and SMARCB1 expression status define two subtypes. Mod Pathol. 2015;28(2):248–260. doi:10.1038/modpathol.2014.100 [PubMed: 25103069]
12. Agaimy A, Rau TT, Hartmann A, Stoehr R. SMARCB1 (INI1)-negative Rhabdoid Carcinomas of the Gastrointestinal Tract. Am J Surg Pathol. 2014;38(7):910–920. doi:10.1097/pas.0000000000000173 [PubMed: 24503755]
13. Strehl JD, Wachter DL, Fiedler J, et al. Pattern of SMARCB1 (INI1) and SMARCA4 (BRG1) in poorly differentiated endometrioid adenocarcinoma of the uterus: Analysis of a series with emphasis on a novel SMARCA4-deficient dedifferentiated rhabdoid variant. Ann Diagn Pathol. 2015;19(4):198–202. doi:10.1016/j.anndiagpath.2015.04.001 [PubMed: 25920939]
14. Jamshidi F, Pleasance E, Li Y, et al. Diagnostic Value of Next-Generation Sequencing in an Unusual Sphenoid Tumor. Oncologist. 2014;19:623–630. [PubMed: 24807916]
15. Agaimy A, Koch M, Lell M, et al. SMARCB1(INI1)-deficient sinonasal basaloid carcinoma: A novel member of the expanding family of SMARCB1-deficient neoplasms. Am J Surg Pathol. 2014;38(9):1274–1281. doi:10.1097/PAS.0000000000000236 [PubMed: 24832165]
16. Bishop JA, Antonescu CR, Westra WH. SMARCB1 (INI-1)-deficient carcinomas of the sinonasal tract. Am J Surg Pathol. 2014;38(9):1282–1289. doi:10.1097/PAS.0000000000000285 [PubMed: 25007146]
17. Agaimy A, Hartmann A, Antonescu CR, et al. SMARCB1 (INI-1)-deficient Sinonasal Carcinoma. A Series of 39 Cases Expanding the Morphologic and Clinicopathologic. Am J Surg Pathol 2017;41(4):458–471. [PubMed: 28291122]
18. Kakkar A, Antony VM, Pramanik R, Sakthivel P, Singh CA, Jain D. SMARCB1 (INI1)- deficient sinonasal carcinoma: a series of 13 cases with assessment of histologic patterns. Hum Pathol. 2019;83:59–67. doi:10.1016/j.humpath.2018.08.008 [PubMed: 30120966]
19. Allison DB, Bishop JA, Ali SZ. Cytopathologic Characteristics of SMARCB1 (INI-1) Deficient Sinonasal Carcinoma: A Potential Diagnostic Pitfall. Diagn Cytopathol. 2016;44(8):700–703. doi:0.1002/dc.23503 [PubMed: 27177850]
20. Allard FD, Bell D, Stelow EB. Cytopathologic features of SMARCB1 (INI-1)-deficient sinonasal carcinoma. Cancer Cytopathol. 2018;126(8):567–574. doi:10.1002/cncy.22020 [PubMed: 29797680]
21. Landa I, Ibrahimpasic T, Boucai L, et al. Genomic and transcriptomic hallmarks of poorly differentiated and anaplastic thyroid cancers. J Clin Invest. 2016;126(3):1052–1066. doi:10.1172/JCI85271 [PubMed: 26878173]

22. Cotzia P, Grounder M. Genetic and Histologic Spectrum of SMARCB1-deficient Carcinomas of the Head and Neck Including Sinonasal Tract, Thyroid and Skin. Lab Investig. 2018;98(suppl 1:474–475.
23. Kadoch C, Copeland RA, Keilhack H. PRC2 and SWI/SNF Chromatin Remodeling Complexes in Health and Disease. Biochemistry. 2016;55(11):1600–1614. doi:10.1021/acs.biochem.5b01191 [PubMed: 26836503]
24. Wilson BG, Wang X, Shen X, et al. Epigenetic antagonism between Polycomb and SWI/SNF complexes during oncogenic transformation. Cancer Cell. 2011;18(4):316–328. doi:10.1016/j.ccr.2010.09.006.Epigenetic
25. Chen Y, Hung M, Li L. EZH2: a pivotal regulator in controlling cell differentiation. Am J Transl Res. 2012;4(4):364–375. [PubMed: 23145205]
26. Alimova I, Birks DK, Harris PS, et al. Inhibition of EZH2 suppresses self-renewal and induces radiation sensitivity in atypical rhabdoid teratoid tumor cells. Neuro Oncol. 2013;15(2):149–160. doi:10.1093/neuonc/nos285 [PubMed: 23190500]
27. Knutson SK, Warholic NM, Wigle TJ, et al. Durable tumor regression in genetically altered malignant rhabdoid tumors by inhibition of methyltransferase EZH2. Proc Natl Acad Sci. 2013;110(19):7922–7927. doi:10.1073/pnas.1303800110 [PubMed: 23620515]
28. Januario T, Ye X, Bainer R, et al. PRC2-mediated repression of SMARCA2 predicts EZH2 inhibitor activity in SWI/SNF mutant tumors. Proc Natl Acad Sci. 2017;114(46):12249–12254. doi:10.1073/pnas.1703966114 [PubMed: 29087303]
29. Wang Y, Chen SY, Karnezis AN, et al. The histone methyltransferase EZH2 is a therapeutic target in small cell carcinoma of the ovary, hypercalcaemic type. J Pathol. 2017;242(3):371–383. doi:10.1002/path.4912 [PubMed: 28444909]
30. https://clinicaltrials.gov/ct2/show/NCT02601950?term=ezh2&rank=4.
31. Cheng DT, Mitchell TN, Zehir A, et al. Memorial Sloan Kettering-Integrated Mutation Profiling of Actionable Cancer Targets A Hybridization Capture-Based Next-Generation Sequencing Clinical Assay for Solid Tumor Molecular Oncology. J Mol Diagnostics. 2015;17(3):251–264. doi:10.1016/j.jmoldx.2014.12.006
32. Zehir A, Benayed R, Shah RH, et al. Mutational landscape of metastatic cancer revealed from prospective clinical sequencing of 10,000 patients. Nat Med. 2017;23(6):703–713. doi:10.1038/nm.4333 [PubMed: 28481359]
33. Kodet R, Newton WA, Sachs N, et al. Rhabdoid tumors of soft tissues: A clinicopathologic study of 26 cases enrolled on the intergroup rhabdomyosarcoma study. Hum Pathol. 1991;22(7):674–684. doi:10.1016/0046-8177(91)90289-2 [PubMed: 1712749]
34. Karnezis AN, Hoang LN, Coatham M, et al. Loss of switch/sucrose non-fermenting complex protein expression is associated with dedifferentiation in endometrial carcinomas. Mod Pathol. 2016;29(3):302–314. doi:10.1038/modpathol.2015.155 [PubMed: 26743474]
35. Agaimy A, Bertz S, Cheng L, et al. Loss of expression of the SWI/SNF complex is a frequent event in undifferentiated/dedifferentiated urothelial carcinoma of the urinary tract. Virchows Arch. 2016;469(3):321–330. doi:10.1007/s00428-016-1977-y [PubMed: 27339451]

Highlights

- SMARCB1-deficient carcinomas of the head and neck show highly variable cytomorphology
- High grade features, including multinucleation, mitoses and necrosis are frequently seen
- “Rhabdoid” cells may be present, but are relatively uncommon
- Most specimens showed no distinct epithelial differentiation

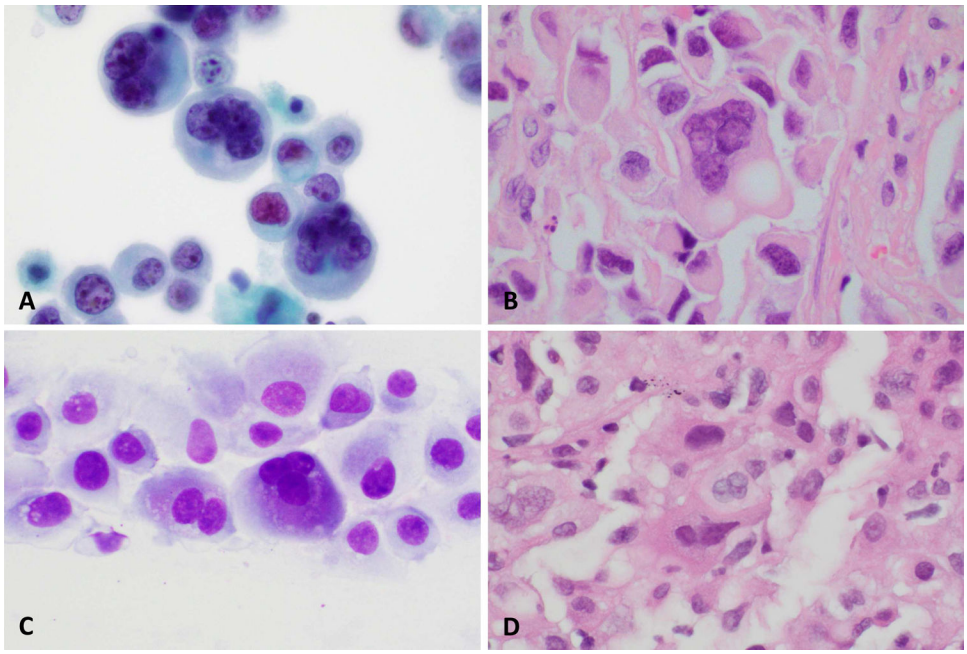

Figure 1.

Multinucleation in a primary thyroid carcinoma shown on Papanicolaou stained monolayer preparation (A) and in the corresponding primary surgical resection specimen (B). Bi- and multinucleation in a fine needle aspiration specimen of a cervical lymph node, unknown primary site (A) and a subsequent liver biopsy (B).

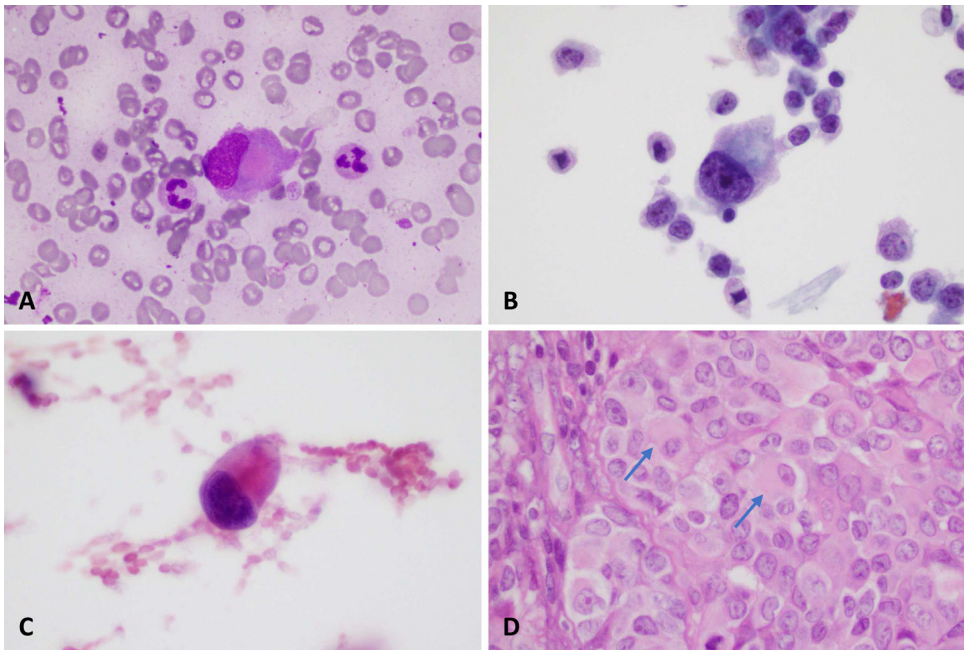

Figure 2.

SMARCB1-deficient sinonasal carcinoma showing rhabdoid cells in DiffQuik (A), Papanicolaou (B), and H&E (C) stained smears. The corresponding surgical resection specimen (D) is also shown.

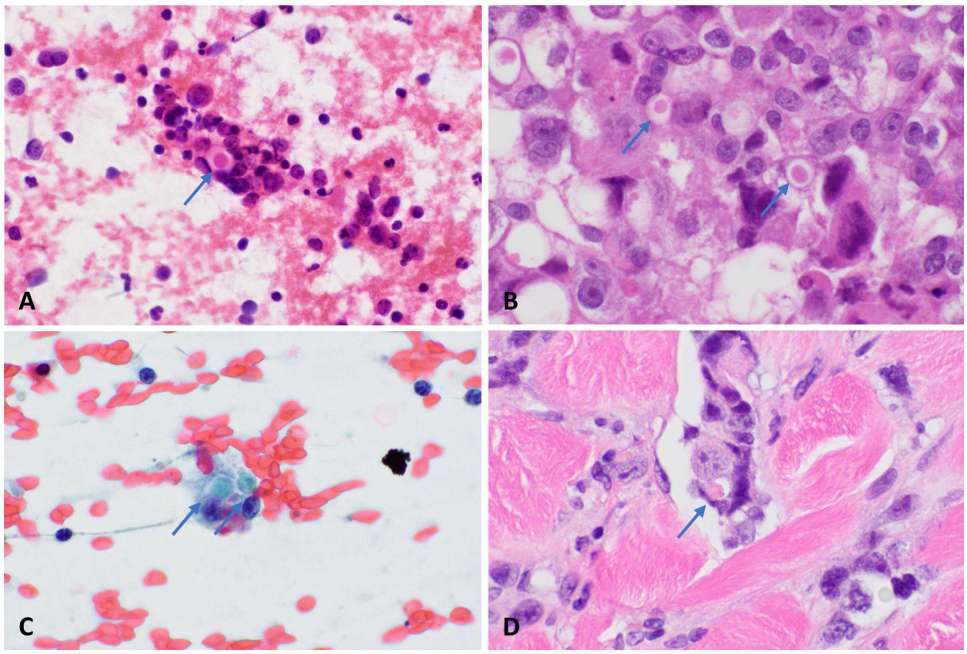

Figure 3.

Dense, eosinophilic cytoplasmic globules in a SMARCB1-deficient sinonasal carcinoma on H&E stained smear (A) and in the primary surgical resection specimen (B). Primary skin carcinoma, shown on Papanicolaou stained smear (C) and primary surgical resection specimen (D) also demonstrates dense, eosinophilic globules.

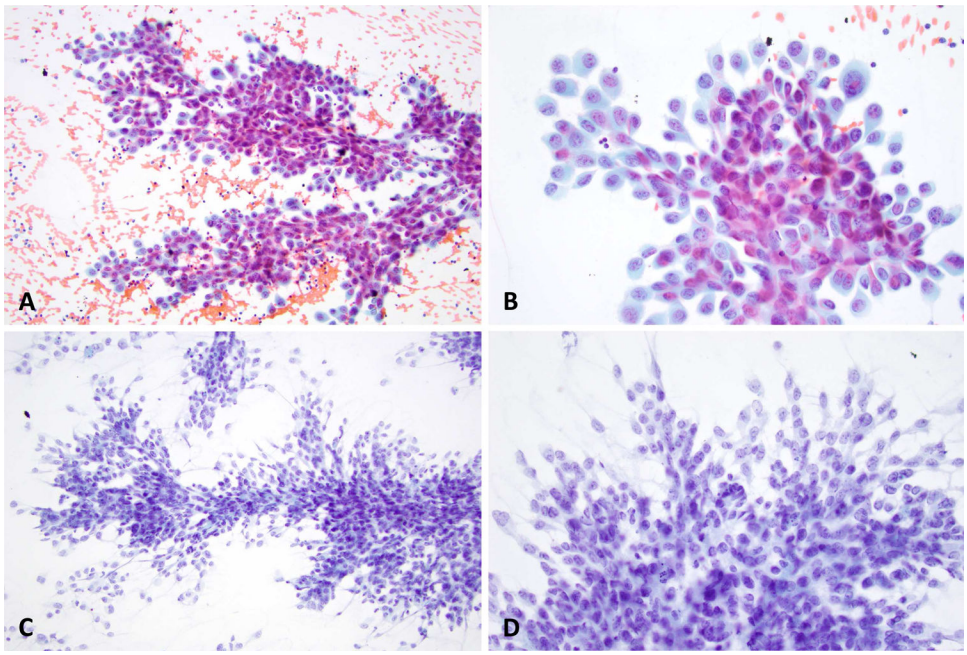

Figure 4.

Two different sinonasal carcinomas demonstrating the two dominant patterns identified in this study; Dense cytoplasm with distinct nuclear borders (A and B) versus delicate cytoplasm with indistinct nuclear borders (C and D).

Table 1.

Patient demographics, primary diagnosis, specimen site and specimen type

	Primary Site	Age	Pathologic Diagnosis	Specimen Site	Specimen Type
1	Sinonasal	53	Poorly differentiated/Undifferentiated carcinoma	Preauricular mass	FNA
2	Sinonasal	54	Poorly differentiated squamous cell carcinoma with basaloid features	Shoulder fluid collection	FNA
3	Sinonasal	54	Poorly differentiated carcinoma with focal glandular and clear cell features	Bone lytic lesion	FNA
4	Sinonasal	66	Poorly differentiated carcinoma, favor adenocarcinoma	Lymph node	FNA
5	Sinonasal	33	Poorly differentiated non-keratinizing squamous cell carcinoma	Lung	FNA and touch prep
6	Sinonasal	79	Poorly differentiated carcinoma with glandular features, SMARCB-1 deficient	Liver	Touch prep and rinse
				Liver	Touch prep and rinse
7	Sinonasal	26	Poorly differentiated carcinoma	Lung	Touch Prep
8	Thyroid	59	Anaplastic carcinoma	Peritoneal fluid	Fluid
9	Thyroid	67	Anaplastic carcinoma	Thyroid	FNA
10	Thyroid	50	Undifferentiated neoplasm admixed with cribriform morular variant of papillary thyroid carcinoma	Lymph node	FNA
				Lung	FNA
11	Skin	18	Poorly differentiated carcinoma	Lymph node	FNA and touch prep
12	Skin	76	Poorly differentiated carcinoma, SMARCB1 (INIl)-deficient	Submental mass	Touch prep and rinse
				Retroauricular mass	Touch prep and rinse
13	Unknown	52	Poorly differentiated carcinoma	Lymph node	FNA
				Liver	Touch prep and rinse
				Lung	BAL
				Lung	Brush

Table 2.

Cytomorphologic features

Results per Specimen	Total N=19		Sinonasal Carcinoma N=8		Thyroid N=4		Skin N=3		Unknown Primary N=4	
Nucleoli	19	100%	8	100%	4	100%	3	100%	4	100%
Mitoses	11	58%	4	50%	3	75%	3	100%	3	75%
Necrosis	13	68%	4	50%	4	100%	3	100%	2	50%
Nuclear grooves/indentations	13	68%	5	63%	4	100%	3	100%	1	25%
Bi-or Multinucleation	16	84%	7	88%	2	50%	3	100%	4	100%
Rhabdoid Cells Present	4	21%	2	25%	2	50%	0	-	0	-
Differentiation										
None	12	47%	6	75%	3	75%	3	100%	0	-
Glandular/Signet Ring	7	37%	2	25%	1	25%	0	-	4	100%
Cytoplasmic inclusions										
Vacuoles	13	68%	5	63%	2	50%	2	67%	4	100%
Eosinophilic bodies	4	21%	2	25%	0	-	1	33%	1	25%
Cytoplasm										
Delicate with indistinct borders	9	47%	4	50%	2	50%	3	100%	4	100%
Dense with distinct borders	10	53%	4	50%	2	50%	0	-	0	-